The effects of GLP-1 receptor agonist on insulin sensitivity
(GLP1 受容体作動薬がインスリン感受性に及ぼす影響についての検討)

Satoru Yamazaki

ABSTRACT

【OBJECTIVE】Liraglutide is an once-daily human glucagon-like peptide-1 (GLP-1) receptor agonists that improves overall glycemic control by stimulating insulin secretion and inhibiting of glucagon secretion. However, the effect of liraglutide on insulin sensitivity has not been fully elucidated. In this study, we therefore investigated the effect of liraglutide on insulin sensitivity and glucose metabolism in male Wistar rats.

【METHOD】Male Wister rats were fed a normal chow diet (NCD) or 60% high fat diet (HFD) for a total 4 weeks. After 3 weeks of feeding, they were injected with liraglutide (0, 0.05, and 0.1 mg/rat) once a day for 7 days, and then euglycemic- hyperinsulinemic clamp studies (at 25 mU/kg/min insulin infusion rate) was performed after a 8-hour fast.

【RESULT】In the NCD fed rats, during the clamp studies, the glucose infusion rate (GIR) required to euglycemia was significantly increased by 17.9% and 14.0% in the 0.05 and 0.1 mg liraglutide group, respectively, compared to in the control group. The clamp hepatic glucose output (cHGO) was significantly decreased by 48.7% and 48.0% in the 0.05 and 0.1 mg liraglutide group, respectively, but insulin-stimulated glucose disposal rate (IS-GDR) was no significant changes in three groups. On the other hand, in the HFD fed rats, during the clamp studies, the GIR was significantly increased by 14.7% and 16.9% in the 0.05 and 0.1 mg liraglutide group, respectively, compared to in the control HFD group. The cHGO was significantly decreased by 51.1% and 42.2% in the 0.05 and 0.1 mg liraglutide group, respectively. And the IS-GDR was significantly increased by 13.7% and 17.8% in the 0.05 and 0.1 mg liraglutide group, respectively. Consistent with the clamp data, the insulin stimulated phosphorylation of Akt and AMPK was enhanced in liver of NCD and HFD fed rats and in skeletal muscle of HFD fed rats. Furthermore, the oil-red stain indicated that liraglutide improved hepatic steatosis.

【CONCLUSION】In normal glucose tolerant state, liraglutide enhances insulin sensitivity in liver but in skeletal muscle. On the other hands, in insulin resistant state, liraglutide improves insulin resistance in liver and muscle. Furthermore, liraglutide improves hepatic steatosis.

INTRODUCTION

Impaired glucose tolerance (IGT) is a pre-diabetic state of hyperglycemia that is associated with insulin resistance and increased risk of cardiovascular disease. IGT may precede type 2 diabetes mellitus by many years. IGT is a risk factor for mortality (1) . Type 2 diabetes is a progressive disease, characterized by insulin resistance and impaired insulin secretion, which leads to chronic hyperglycemia and increased risk of micro- and(1) macro-vascular complications (2). Insulin resistance, which is characterized by the impaired ability of insulin to inhibit glucose output from the liver and to promote glucose uptake in muscle (2), is frequently found in individuals with impaired glucose intolerance (IGT). Insulin resistance is the central component defining the metabolic syndrome, and is present in a constellation of abnormalities, including obesity, hypertension, glucose intolerance, and dyslipidemia (3). Therefore, it is very important of the treatment regarding of insulin resistance in Type 2 diabetes.

Glucagon-like peptide-1 (GLP-1) is an incretin hormone secreted from the gastrointestinal endocrine cells in response to food intake. GLP-1 can stimulate endogenous insulin secretion and decrease glucagon release in a glucose-dependent manner (4), and it was indicated in early studies that GLP-1 treatment resulted in the reduction of fasting and postprandial plasma glucose concentrations in patients with type 2 diabetes (5). GLP-1 has also been shown to have trophic effects on the β-cell (6), and one mechanism by which GLP-1 has also shown to be responsible for the expansion of β-cell mass, is inhibition of apoptosis (7). The effect of GLP-1 on apoptosis appears to be mediated by the GLP-1 receptor, and the expression of the GLP-1 receptor in a non-pancreatic cell line renders these cells sensitive to the inhibition of programmed cell death by GLP-1 (8).

The receptor for GLP-1 is a member of the family of G-protein-coupled receptors, comprising an extracellular N-terminal domain containing six conserved cysteine residues and a core domain comprising the seven transmembrane helices and interconnecting loop regions (9). Binding of GLP-1 to the GLP-1 receptor increases accumulation of intracellular cyclic adenosine monophosphate (cAMP) (10). The GLP-1 receptor has been localized to a wide variety of tissues, including stomach, duodenum, exocrine pancreas, brainstem, thalamus, hypothalamus, hippocampus, heart, lung, and kidney, as well as the pancreatic islets cells (11). Furthermore, GLP-1

binding sites have also been found in myocytes, adipocytes, and hepatocytes.

The discovery of GLP-1 outside of the islets provides strong evidence that this hormone may exhibit many extra-islet effects, and corroborates other studies which demonstrate the physiological effects of GLP-1 in a variety of extra-pancreatic tissues, such as inhibition of gastrointestinal motility, appetite suppression, induction of diuresis, hypotensive effect, and myocardial protection during myocardial infarction(11) (12) (13) (14) (15). And, it has been reported that the glycogenic effect of GLP-1, which effect is independent of insulin and expected to lower plasma glucose, has been found in rat hepatocytes and rat skeletal muscle (10) (16) (17) (18). These findings from these studies therefore raise the possibility that GLP-1 may play wider physiological roles than those currently understood, and that this hormone demonstrates beneficial effect in states of insulin resistance. However, the effects of GLP-1 on insulin sensitivity remain to be established.

Liraglutide is an analogue of human GLP-1, with 97% homology to the human GLP-1 and is prescribed as a once-daily treatment for type 2 diabetes, and functions to improve overall glycemic control by both stimulating insulin secretion, and inhibiting glucagon secretion. Clinical trials of liraglutide in patients with type 2 diabetes have demonstrated improved levels of both fasting and postprandial glucose (15). And it has been reported that liraglutide is associated with weight loss, and decreasing of the homeostasis model assessment insulin resistance values (HOMA-IR) in clinical trials (19) (20). Therefore, it is expected that liraglutide improves insulin resistance.

While it has been recorded that liraglutide has excellent actions for the blood glucose management in type 2 diabetes, including of reduction of HbA1c and fasting plasma glucose values in both basic research and clinical trial, the effects of liraglutide on insulin resistance, which is one of the fundamental disease states leading to diabetes and cardiovascular events, has not been fully elucidated. Therefore, we investigated the effect of liraglutide on both insulin sensitivity and glucose metabolism, by examining of the effect of liraglutide under both normal glucose tolerance and insulin resistance. In this study, we selected the high fat diet (HFD) feeding rats as insulin resistance model rats, considering previous reports which demonstrated that HFD-feeding involved insulin resistance (21) (22).

RESEARCH DESIGN AND METHODS

Materials

Male Wistar rats were procured from Charles River Laboratory Japan, Inc. (Kanagawa, Japan). Liraglutide and insulin (Novolin R) were purchased from Novo Nordisk (Copenhagen, Denmark). HFD (60% w/w, #D12492) was purchased from Research Diet Inc. (New Brunswick, NJ, USA). The catheter (Micro-Renathane MRE-033, 0.033 cm in OD and 0.014 cm in ID) was purchased from Braintree Scientific (Braintree, MA, USA). D-[3-3H] glucose was purchased from PerkinElmer Inc. (Waltham, MA, USA). Pentobarbital was purchased from Kyoritsu Pharmaceutical Co. (Tokyo, Japan). The 50% dextrose was purchased from Otsuka Pharmaceutical Co. (Tokushima, Japan). Polyvinylidine difluoride (PVDF) transfer membranes were purchased from Millipore Corp (Bedford, MA, USA). Anti-phospho-specific Akt (Ser473), phospho-AMP-activated protein kinase (AMPK) (Thr172), Akt, AMPK and β-actin antibodies were purchased from Cell Signaling Technology (Boston, MA, USA). Horseradish peroxidase-conjugated secondary antibody was purchased from Santa Cruz Biotechnology (Santa Cruz, CA, USA). TRIzol reagent was purchased from Invitrogen Life Technologies (Carlsbad, CA, USA). The RNeasy kit was purchased from QIAGEN Inc. (Valencia, CA, USA). iScript cDNA Synthesis Kit and iQ SYBR Green Supermix were purchased from Bio-Rad Laboratories (Richmond, CA, USA). All other reagents were purchased from Sigma (St. Louis, MO, USA).

Animal studies

Six-week-old male Wistar rats (Charles River Laboratory Japan, Inc.) were housed individually under controlled light/dark (12/12 hours) and temperature conditions (25 ˚C), and had free access to water and a normal chow diet (NCD) or 60% HFD (Research Diet Inc.) for a total of 4 weeks. The rats received a fresh diet every 3 days, and food consumption rats, and body weight gains, were monitored every 3 days. After observing the indicated chow diet for 3 weeks, the rats were implanted with 3 catheters (Micro-Renathane MRE-033, 0.033 cm in OD and 0.014 cm in ID; Braintree Scientific, Braintree, MA), as previously described (23). In brief, 2 catheters were placed into the right jugular vein, and another one was placed into the left carotid artery under a single-dose anesthesia of pentobarbital 50 mg/kg (Kyoritsu Pharmaceutical Co.) administered intraperitoneally. Catheters

were tunneled subcutaneously, exteriorized at the back of the neck, and filled with heparinized saline. The jugular and carotid catheters were used for infusion and blood sampling, respectively. The rats were subsequently injected subcutaneously with normal saline or liraglutide (0.025, 0.05, and 0.1 mg) per rat, once a day for 7 days (Fig. 1). While the half-life of liraglutide in human is around 15 hours, the one in rats is around 3 hours, and we selected 0.025 mg/rat/day, 0.05 mg/rat/day, and 0.10 mg/rat/day as dosage of liraglutide in the light of previous reports with rats (24) (25). All procedures were performed in accordance with the Guide for Care and Use of Laboratory Animals of the NIH and were approved by the Animal Subjects Committee of the Fukushima Medical University, Japan.

Glucose tolerance tests and euglycemic-hyperinsulinemic clamp procedures

After 7 days of daily liraglutide injections, glucose tolerance and insulin sensitivity was assessed by using an intravenous glucose tolerance test (iv-GTT) and euglycemic-hyperinsulinemic clamp. The rats were fasted for 8 hours before the start of all experiments.

For the iv-GTT, the rats were injected into the jugular vein with dextrose (50% dextrose; Otsuka Pharmaceutical Co.), at 2 g/kg body weight. Blood samples were then collected at time 0, 15, 30, 60, 90, and 120 min post-injection, from the carotid artery.

The euglycemic-hyperinsulinemic clamp experiments began with a constant infusion (0.04 μCi/min) of D-[3-3H] glucose (New England Nuclear). After 120 min of tracer equilibration and basal sampling at time -10 min, and 0 min, glucose (50% dextrose, variable infusion; Otsuka Pharmaceutical Co.) and tracer (0.12 μCi/min) plus insulin (25 mU/kg/min, Novolin R; Novo Nordisk) were infused into the jugular vein as previously described (26, 27). Small blood samples (60 μl) were drawn at 10-min intervals and immediately analyzed for glucose (Compact Electrode Blood Sugar Analyzer Antsense: HORIBA Ltd, Kyoto, Japan) to maintain the integrity of the glucose clamp throughout the duration of the experiment. Blood samples were taken at -120 min (start of experiment), -10 min and 0 min (basal), and 110 min and 120 min (end of experiment), for determination of glucose specific activity, and insulin content, to ensure accuracy, these basal and terminal samplings were performed twice, with the 10-minute interval between sampling. Before obtaining the terminal blood specimen, the establishment of

steady-state conditions at the end of the clamp was confirmed by measuring blood glucose levels every 10 minutes, providing assurance that a steady state for glucose infusion and plasma glucose levels was maintained for a minimum of 20 minutes before final sampling. We define a steady-state blood glucose concentration as one in which the blood glucose concentration and infusion rate fluctuate by 3 mg/dl or less, and by 5% or less, respectively, over 10 minutes. All blood samples were immediately centrifuged, and plasma was stored at -80 ºC for subsequent analysis. After terminal blood sampling at 120 min, animals were promptly euthanized with pentobarbital (180 mg/kg). Tissues were harvested and immediately frozen in liquid nitrogen and stored at -80 ºC for subsequent metabolic analysis.

Analytical procedures

Rat insulin, human insulin, glucagon, adiponectin, free fatty acid, triglyceride (TG), total cholesterol (TC), and high-density lipoprotein cholesterol (HDL-C) were analyzed by a private laboratory (SRL Laboratory, Tokyo, Japan). Plasma glucose specific activity was measured in duplicate after zinc sulfate and barium hydroxide deproteinization.

Immunoblotting analysis

Liver, red quadriceps muscle, and white adipose tissue used for metabolic analyses were harvested from animals immediately after euthanasia. They were then rinsed several times in cold saline to remove blood, and then frozen in liquid nitrogen, and stored at -80 ºC. Care was taken to avoid harvesting sections of the liver lobes containing large blood vessels. Tissues were homogenized in liquid nitrogen and lysed in buffer containing phosphatase and protease inhibitors (Complete Mini; Roche Applied Science), according to the protocol of the manufacturer. Tissue protein concentrations were determined by the BCA protein assay, using the BCA reagent (Thermo Fisher Scientific Inc.). Equal amounts of protein were separated by 10% sodium dodecyl sulfate-polyacrylamide gel electrophoresis (SDS-PAGE), and transferred to PVDF membranes (Immobilon; Millipore), which were then blocked with ImmunoBlock (DS Pharma Biomedical Co. Ltd.) overnight. The membranes were probed firstly with primary Akt, phospho-Akt (Ser473), AMPK, and phospho-AMPK (Thr172) antibodies (Cell Signaling Technology), followed by probing with a horseradish peroxidase-conjugated secondary

antibody (Santa Cruz Biotechnology). The immunocomplexes were visualized with ECL western blotting detection reagents (Amersham; GH Healthcare, UK). ß-actin served as an internal control protein. Band intensities were quantified by densitometry using the Image-J software (NIH, Bethesda, MD, USA).

Quantitative real time RT-PCR analysis

Total RNA samples were extracted from the liver tissues with TRIzol reagent (Invitrogen Life Technologies), and further purified using the RNeasy kit using RNase-free DNase I treatment according to the manufacturer's instructions. Total RNA (1 µg) was then reverse-transcribed using iScript cDNA Synthesis Kit according to the manufacturer's instructions (Bio-Rad Laboratories). Quantitative real-time PCR was performed with a Bio-Rad system using iQ SYBR Green Supermix and specific primer pairs selected with Primer Express software (Applied Biosystems). The relative mass of specific RNAs was calculated by the comparative cycle of threshold detection method according to the manufacturer's instructions.

Histological examination.

A portion of liver was fixed with 10% formalin and embedded in paraffin. Sections of 3-µm were cut and stained with hematoxylin and eosin for examination of liver histology (BX-50, Olympus Corporation, Tokyo, Japan). To examine lipid accumulation, 6-µm frozen sections were stained with Oil Red O.

Calculations

HOMA-IR was calculated from the fasting concentrations of insulin and glucose using the following formula fasting plasma insulin (ng/ml) × fasting plasma glucose (mg/dl) /405. Hepatic glucose output (HGO) and glucose disposal rate (GDR) were calculated for the basal period and steady-state portion of the glucose clamp using the Steele equation for steady-state conditions (28). The insulin-stimulated GDR (IS-GDR) reflects the ability of insulin to increase GDR above the basal value, and it is calculated by subtracting each animal's basal HGO value from the final GDR achieved at the end of the clamp period (IS-GDR = total GDR - basal HGO value). Data

are presented as mean ± SEM. Statistical significance was tested with repeated measures using ANOVA. Statistical significance was defined as $P < 0.05$.

RESULTS

Overall animal characteristics

The effect of liraglutide was examined in both NCD-fed and HFD-fed male Wister rats. Male Wistar rats were fed a NCD or HFD for 3 weeks, and were subsequently injected subcutaneously with the indicated once-daily dosage of liraglutide for 7 days. Table 1 illustrates some of the general characteristics of the liraglutide and control group in the basal state after injection of liraglutide for 7 days. Compared with the control group (n = 25), in the NCD-fed rats, body weight was significantly decreased in a dose-dependent manner by 5.1% ($P < 0.05$), 13.5% ($P < 0.05$), and 19.9% ($P < 0.05$), in liraglutide groups receiving 0.025 (n = 8), 0.05 (n = 25), and 0.1 mg (n = 10) of the drug, respectively. In the fasting state, plasma glucose levels were significantly lower ($P < 0.05$) in the liraglutide group (0.025 mg/day: n = 8, 0.05 mg/day: n = 12, 0.10 mg/day: n = 10) than in the control group (n = 12), and HOMA-IR, which evaluates the insulin sensitivity, was significantly decreased ($P < 0.05$) in the liraglutide group (0.05 mg/day: n = 12) compared to the control group (n = 12), suggesting an improvement of insulin sensitivity after the 7-day regimen of daily liraglutide injections (Table 1).

Glucose tolerance test

After the 7-day regimen of daily liraglutide injections, iv-GTTs were performed on rats that had been fasted for 8 hours and then injected with glucose (2 g/kg body weight) into the jugular vein. As seen in Fig. 2A, the fasting blood glucose levels and the blood glucose levels after the glucose load were significantly lowered in liraglutide groups (0.05 mg/day: n = 4, 0.10 mg/day: n = 3) after 30 and 60 minutes ($P < 0.05$), compared with the control group (n = 4).

Euglycemic-hyperinsulinemic clamp

To directly examine the quantitative effect of liraglutide on insulin sensitivity, we next subjected both groups of rats to euglycemic hyperinsulinemic clamping. These experiments were performed after the

7-day regimen of daily liraglutide injections at maximal insulin infusion rate (25 mU/kg/min). Steady-state glucose and insulin levels during the clamp studies were the almost identical in both groups, as shown in Table 1. During these studies, we measured insulin stimulation of whole-body GDR and suppression of HGO. As seen in Fig. 2B, the glucose infusion rate (GIR) required to achieve euglycemia was significantly increased by 8.5% ($P < 0.05$), 17.9% ($P < 0.01$), and 14.0% ($P < 0.05$) in group injected with 0.025 (n = 8), 0.05 (n = 10), and 0.1 mg (n = 7) liraglutide respectively, compared with the control group (n = 9) showing enhanced overall insulin sensitivity. To assess the insulin-stimulated component of glucose disposal, the IS-GDR was calculated. As shown by Fig. 2C, the IS-GDR was not significantly different among those groups. Basal HGO was significantly decreased by 19.5% ($P < 0.05$), 20.1% ($P < 0.01$), and 19.0% ($P < 0.05$) in groups injected with 0.025 (n = 8), 0.05 (n = 10), and 0.1 mg (n = 7) liraglutide respectively, compared with the control group (n = 9) (Fig. 2D). During the clamp studies, insulin inhibition of HGO was significantly enhanced by 48.1% ($P < 0.01$), 48.7% ($P < 0.01$), and 48.0% ($P < 0.05$) in groups injected with 0.025 (n = 8), 0.05 (n = 10), and 0.1 mg (n = 7) liraglutide injection groups, respectively, compared with the control group (n = 9) (Fig. 2E), suggesting that liraglutide augments hepatic insulin sensitivity in NCD-fed rats.

HFD feeding studies

We also studied liraglutide-treated animals administered with a 4-week long HFD to assess the potential protective effects of liraglutide on the development of insulin resistance. At the basal state in control animals, HFD feeding (n = 30) led to a 31% increase in body weight and a 13% increase in fasting insulin levels, but no change in fasting plasma glucose levels, compared with NCD feeding (n = 25) (Tables 1 and 2). When euglycemic-hyperinsulinemic clamp studies were performed in HFD-fed control animals (n = 11), GIRs required to maintain euglycemia were decreased by 25% ($P < 0.05$) (Fig. 3B) compared with the NCD-fed control animals (n = 9) (Fig. 2B); these results are consistent with the HFD-induced insulin-resistant state. In the HFD-fed rats, body weight was decreased by 9.8% in the 0.1 mg liraglutide injection group (n = 8), compared with the HFD-fed control group (n = 11) (Table 2). After the 7-day regimen of once-daily liraglutide injections, iv-GTTs were performed on rats fasted for 8

hours then injected with glucose (2k/kg body weight) into the jugular vein. As seen in Fig. 3A, the fasting blood glucose levels and after blood glucose levels after the glucose load were significantly decreased in the liraglutide group (0.05 mg/day: n = 5, 0.10 mg/day: n = 5) at 30, 60, and 90 minutes post-glucose injection ($P < 0.05$), compared with the control group (n = 8). Euglycemic-hyperinsulinemic clamp studies at maximal insulin infusion rate (25 mU/kg/min) were also performed on rats following the 7-day regimen of once-daily liraglutide injections. Steady-state glucose and insulin levels during the clamp studies were the almost identical across all groups, as shown in Table 2. During these studies, we also measured insulin stimulation of whole-body GDR and suppression of HGO. As shown by Fig. 3B, the GIR required to achieve euglycemia was significantly increased by 21.6% ($P < 0.01$), 14.7% ($P < 0.05$), and 16.9% ($P < 0.05$) in the 0.025 (n = 8), 0.05 (n = 8) and 0.1 mg (n = 8) liraglutide group, respectively, in HFD-fed rats, compared with the HFD-fed control rats (n = 11); thus showing improved overall insulin resistance. As seen in Fig. 3C, the IS-GDR was significantly increased by 23.9% ($P < 0.01$), 13.7% ($P < 0.05$), and 17.8% ($P < 0.05$) in the 0.025 (n = 8), 0.05 (n = 8), and 0.1 mg (n = 8) liraglutide groups, respectively, in HFD-fed rats, compared with the HFD-fed control rats (n = 11); thus showing improved the peripheral insulin resistance. Basal HGO was also significantly decreased by 16.6% ($P < 0.01$), and 15.9% ($P < 0.01$) in the 0.05 (n = 8), and 0.1 mg (n = 8) liraglutide groups, respectively, in the HFD-fed rats, compared with the HFD-fed control group (n = 11) (Fig. 3D). During the clamp studies, insulin inhibition of HGO was significantly enhanced by 26.4% ($P < 0.05$), 51.1% ($P < 0.01$), and 42.2% ($P < 0.01$) in the 0.025 (n = 8), 0.05 (n = 8), and 0.1 mg (n = 8) liraglutide groups, respectively, compared with the control group (n = 11) (Fig. 3E), suggesting that liraglutide improves hepatic insulin sensitivity in HFD-fed rats.

Insulin signaling studies

To investigate the potential cellular mechanisms underlying the liraglutide-induced increase in insulin sensitivity, we obtained skeletal muscle, epididymal adipose tissue, and liver samples from rats in the basal and terminal stages of the euglycemic-hyperinsulinemic clamp studies; the latter samples represent the fully insulinized state at the termination of the glucose clamp study. These tissues were then homogenized and subjected to

immunoblotting, following which we then measured the phosphorylation of Akt (Ser473), which is the most critical molecule in the insulin signaling (29). In addition, since AMPK signaling affects insulin-sensitive glucose metabolism (30) and since AMPK can act upstream of Akt signaling (31), we also measured AMPK phosphorylation (Thr172) in skeletal muscle, epididymal adipose tissue, and liver samples obtained from NCD-fed and HFD-fed rats at the terminal stage of the euglycemic-hyperinsulinemic studies. As shown in Fig. 4A, insulin led to a marked stimulation of Akt phosphorylation in all three tissue types from NCD-fed control rats. In NCD-fed rats receiving liraglutide (n = 4), this effect of Akt phosphorylation at Ser473 was augmented by 64% ($P < 0.05$) in liver, but neither in skeletal muscle nor epididymal adipose tissue, compared with NCD-fed rats receiving normal saline (n = 4). Furthermore, AMPK phosphorylation at Thr172 was also augmented by 51% ($P < 0.05$) in liver of NCD-fed liraglutide-treated rats (n = 4), while AMPK protein content remained unchanged, compared with NCD-fed rats receiving normal saline (n = 4) (Fig. 4B). In contrast, both AMPK phosphorylation and protein content were unchanged in skeletal muscle and epididymal adipose tissue of NCD-fed liraglutide-treated rats. On the other hand, the insulin-stimulated phosphorylation of Akt in liver and skeletal muscle of HFD-fed liraglutide-treated rats (n = 4), was increased by 40% ($P < 0.05$) and 34% ($P < 0.05$), respectively, but showed no change in epididymal adipose tissue, compared with HFD-fed rats receiving normal saline (n = 4) (Fig. 4C). Furthermore, AMPK phosphorylation at Thr172 in liver and skeletal muscle of HFD-fed liraglutide-treated rats (n = 4) was also augmented by 90% ($P < 0.05$) and 71% ($P < 0.05$), respectively, while AMPK protein content remained unchanged, compared with HFD-fed rats receiving normal saline (n = 4) (Fig. 4D). In contrast, AMPK phosphorylation and protein content were unchanged in epididymal adipose tissue of HFD-fed liraglutide-treated rats (n = 4), compared with HFD-fed rats receiving normal saline (n = 4) (Fig. 4D). Overall, these data are consistent with the results from euglycemic-hyperinsulinemic clamp data.

Gluconeogenic and lipogenic genes in the liver

To investigate the molecular mechanisms of liraglutide-induced increases in insulin sensitivity, we performed qRT-PCR analysis on total RNA from liver tissue samples of NCD-fed and HFD-fed rats at the terminal stages of

the euglycemic-hyperinsulinemic experiments. We first measured the expression levels of glucose-6-phophatase (G6pase), which is a key enzyme in the gluconeogenic pathway. The expression levels of G6pase were significantly decreased by 59% ($P < 0.05$) in liver of NCD-fed liraglutide-treated rats ($n = 6$) compared with those of NCD-fed control rats ($n = 6$), and by 51% ($P < 0.05$) in liver of HFD-fed liraglutide-treated rats ($n = 6$) compared with those of HFD-fed control rats ($n = 6$) (Fig. 5A). These findings indicate that liraglutide suppresses gluconeogenesis in the liver during both normal glucose tolerance, and insulin resistant states.

Next, we measured the expression levels of fatty acid synthase (Fas), acetyl-CoA carboxylase (Acc), ATP citrate lyase (Acl), stearoyl-CoA desaturase (Scd)-1, and sterol regulatory element-binding protein (Srebp)-1c in the liver of NCD-fed and HFD-fed rats at the terminal stage of the euglycemic-hyperinsulinemic experiments. The expression levels of Fas, Acc, Acl, Scd-1, and Srebp-1c, were significantly decreased by 87% ($P < 0.05$), 81% ($P < 0.05$), 77% ($P < 0.05$), 91% ($P < 0.05$), and 76% ($P < 0.05$), respectively, in the liver of NCD-fed liraglutide-treated rats ($n = 6$) compared with those of NCD-fed control rats ($n = 6$), and by 36% ($P < 0.05$), 60% ($P < 0.05$), 63% ($P < 0.05$), 81% ($P < 0.05$), and 79% ($P < 0.05$), respectively, in the liver of HFD-fed liraglutide-treated rats ($n = 6$) compared with those of HFD-fed control rats ($n = 6$) (Figs. 5B, 5C, 5D, 5E, and 5F).

The expression of GLP-1 receptor in liver

To confirm the expression of the GLP-1 receptor in liver, we performed qRT-PCR analysis on total RNA from liver tissue samples of NCD-fed and HFD-fed rats at the terminal stages of the euglycemic-hyperinsulinemic experiments. The expression levels of GLP-1 receptor were not significantly different among with and without liraglutide-injection in both NCD-fed and HFD-fed rats (Fig. 6).

Macroscopic and histological analyses of liver

We observed the characteristics of the rat livers in each group on both a macroscopic scale, as well as performing histological analyses on the HE and oil red O stained tissues. Gross morphological differences in the livers were shown in Fig. 7A, where lipid accumulation in liver resulted in pale discoloration. As Fig. 7B shows, HFD consumption increased liver lipid

content, which was significantly attenuated by liraglutide treatment. This finding was further confirmed by assessment of lipid accumulation using oil red O staining (Fig. 7B). These results indicated that liraglutide treatment reduced the development of hepatic steatosis.

Correlation diagram between GIR and body weight

The liraglutide-treated rats exhibited significantly lower body weights compared with the control rats. To assess whether the effects of augmented insulin sensitivity by liraglutide treatment were dependent on the reduction of body weight, we examined the correlation between body weight and GIR. Body weight was not correlated with GIR in both NCD-fed and HFD-fed rats injected with liraglutide (Figs. 8A and 8B). Moreover, in HFD-fed rats, the regression line of the liraglutide group was located superior to the control group, suggesting that the effects of augmented insulin sensitivity by liraglutide treatment are independent of the reduction of body weight (Fig. 8B).

DISCUSSION

In this in vivo study, we demonstrated the acute effects of the GLP-1 agonist, liraglutide, in male Wistar rats administered with a short (7-day) regimen of liraglutide injections. Our data revealed that in rats, liraglutide, which binds to the GLP-1 receptor, increased glucose tolerance, augmented insulin sensitivity, suppressed the expression of lipogenic enzymes, and ameliorated hepatic steatosis.

The GLP-1 receptor is known to be widely expressed being found in pancreatic islets, kidney, lung, heart, and multiple regions of the peripheral and central nervous system (32). Furthermore, it has been reported that the receptor is present on human hepatocytes where it has a direct role in improving hepatic steatosis (33, 34). In our studies of male Wistar rats, we confirmed the expression of the GLP-1 receptor in liver tissue at the mRNA level. And it has reported that chronic elevated endogenous GLP-1 increased cAMP, which was regulated by binding of GLP-1 to GLP-1 receptor (10), and suppressed hepatic lipogenesis via AMPK in vivo study with transgenic rats (35), therefore we expected that liraglutide, one of GLP-1 analog using widely in clinical, enhanced the activation of AMPK through GLP-1 receptor in liver. Actually, our data in the correlation diagram between GIR and body

weight and insulin signaling studies revealed that the effect on insulin sensitivity of liraglutide was independent of the reduction of body weight, and activated AMPK in liver.

AMPK is a serine/threonine kinase that functions as an intracellular energy sensor and is involved in the modulation of glucose and fatty acid metabolism (36). The activation of AMPK in liver increases the insulin-suppressibility of hepatic glucose output and enhances insulin sensitivity in liver (37). For example, Metformin, which is an anti-diabetic drug both activates AMPK (38), and inhibits the expression of G6Pase, which is one of the key metabolic enzymes in gluconeogenesis and is downstream of AMPK, thus decreasing hepatic glucose production (39). This study showed that liraglutide enhanced the activation of AMPK in liver (Fig. 4B), suppressed the expression of G6pase (Fig. 5A), and suppressed HGO (Fig. 2E and 3E), suggesting that liraglutide promoted insulin sensitivity via AMPK-activation in the liver.

In this study, it was also shown that liraglutide, suppresses lipogenic enzymes such as Fas, Acc, Acl and Scd-1 in liver from both NCD-fed and HFD-fed rats (Fig. 5). Additionally, it was revealed that liraglutide improved the hepatic steatosis in HFD-fed groups according to oil red staining of liver tissue (Fig. 7C). Accumulation of lipids in peripheral tissues, such as pancreatic β-cells, liver, heart, and skeletal muscle, leads to lipotoxicity, a process that contributes substantially to the pathophysiology of insulin resistance, type 2 diabetes, hepatic steatosis and heart failure (40). It is also known that hepatic steatosis increases basal hepatic glucose production and impairs the hepatic insulin action (41). Srebps, form a well-known family of transcription factors that regulate lipid homoeostasis. Srebp-1c, which is a member of the Srebp family, controls the transcription and expression of lipogenic enzymes such as Fas and Scd-1 in liver, and the suppression of Srebp-1c improves hepatic steatosis (42, 43). Therefore, Srebp-1c is regarded as key molecule in hepatic steatosis and insulin resistance, and in this study, liraglutide actually decreased the expression of Srebp-1c in liver (Fig. 5F). It has been shown that the AMPK activation suppresses the expression of Acc and Fas via down-regulation of Srebp-1c (44), considering which our study indicates that the effects of liraglutide in suppressing lipogenesis are based on AMPK activation. Our findings thus suggest that liraglutide is able to improve insulin resistance and hepatic steatosis via suppression of the

lipogenic enzymes that are induced by activation of AMPK in liver.

Additionally, we demonstrated that liraglutide significantly enhanced the activation of AMPK in the skeletal muscle of HFD-fed rats (Fig. 4D). The activation of AMPK increases the expression of GLUT4 in muscle (45), and stimulates the glucose uptake into muscle cells (46). In this study, liraglutide enhanced the IS-GDR, indicating that liraglutide increased the glucose uptake via AMPK activation in skeletal muscle, leading to improve insulin resistance.

Through this study, we have shown that in normal glucose metabolism states, such as NCD-fed rats, liraglutide enhances insulin sensitivity in liver but not in skeletal muscle. We have also demonstrated that in diet-induced insulin resistant states, such as those simulated in HFD-fed rats, liraglutide improves insulin resistance in both liver and skeletal muscle. Furthermore, liraglutide also improves fatty liver in diet-induced insulin resistant states.
In conclusion, we demonstrated that liraglutide enhances insulin sensitivity in liver via an AMPK dependent pathway and improves hepatic steatosis. We thus provide a novel mechanistic explanation for the glucose lowering effects of liraglutide in individual with diabetes. Furthermore, liraglutide might provide useful target for therapeutic agent intended to hepatic steatosis in patients with obesity and type 2 diabetes.

ACKNOWLEDGMENTS

I thanked Tsuyoshi Watanabe MD, PhD and Hiroaki Satoh MD, PhD for expert assistance, Hiroko Ohashi and Atsuko Hashimoto for excellent technical assistance.

FOOTNOTES

The abbreviations used are: normal chow diet (NCD); high fat diet (HFD); glucagon-like peptide-1 (GLP-1); glucose infusion rate (GIR); basal hepatic glucose output (bHGO);clamp hepatic glucose output (cHGO); insulin stimulated glucose disposal rate (IS-GDR); AMP-activated protein kinase (AMPK); fatty acid synthase (FAS); acetyl-CoA carboxylase (ACC); ATP citrate lyase (ACL); stearoyl-CoA desaturase 1 (SCD-1); liraglutide (Lira)

REFERENCES

1. Malin SK, Nightingale J, Choi SE, Chipkin SR, and Braun B. Metformin modifies the exercise training effects on risk factors for cardiovascular disease in impaired glucose tolerant adults. *Obesity.* 2013;21(1):93-100.
2. Olefsky JM, and Glass CK. Macrophages, inflammation, and insulin resistance. *Annual review of physiology.* 2010;72(219-46.
3. Flier JS. Obesity wars: molecular progress confronts an expanding epidemic. *Cell.* 2004;116(2):337-50.
4. Lovshin JA, and Drucker DJ. Incretin-based therapies for type 2 diabetes mellitus. *Nature reviews Endocrinology.* 2009;5(5):262-9.
5. Chia CW, and Egan JM. Incretin-based therapies in type 2 diabetes mellitus. *The Journal of clinical endocrinology and metabolism.* 2008;93(10):3703-16.
6. Wang Y, Perfetti R, Greig NH, Holloway HW, DeOre KA, Montrose-Rafizadeh C, Elahi D, and Egan JM. Glucagon-like peptide-1 can reverse the age-related decline in glucose tolerance in rats. *The Journal of clinical investigation.* 1997;99(12):2883-9.
7. Farilla L, Bulotta A, Hirshberg B, Li Calzi S, Khoury N, Noushmehr H, Bertolotto C, Di Mario U, Harlan DM, and Perfetti R. Glucagon-like peptide 1 inhibits cell apoptosis and improves glucose responsiveness of freshly isolated human islets. *Endocrinology.* 2003;144(12):5149-58.
8. List JF, and Habener JF. Glucagon-like peptide 1 agonists and the development and growth of pancreatic beta-cells. *American journal of physiology Endocrinology and metabolism.* 2004;286(6):E875-81.
9. Mann R, Nasr N, Hadden D, Sinfield J, Abidi F, Al-Sabah S, de Maturana RL, Treece-Birch J, Willshaw A, and Donnelly D. Peptide binding at the GLP-1 receptor. *Biochemical Society transactions.* 2007;35(Pt 4):713-6.
10. Wheeler MB, Lu M, Dillon JS, Leng XH, Chen C, and Boyd AE, 3rd. Functional expression of the rat glucagon-like peptide-I receptor, evidence for coupling to both adenylyl cyclase and phospholipase-C. *Endocrinology.* 1993;133(1):57-62.
11. Ahren B. GLP-1 and extra-islet effects. *Hormone and metabolic research = Hormon- und Stoffwechselforschung = Hormones et metabolisme.* 2004;36(11-12):842-5.

12. Holst JJ. The physiology of glucagon-like peptide 1. *Physiological reviews.* 2007;87(4):1409-39.
13. Elahi D, Egan JM, Shannon RP, Meneilly GS, Khatri A, Habener JF, and Andersen DK. GLP-1 (9-36) amide, cleavage product of GLP-1 (7-36) amide, is a glucoregulatory peptide. *Obesity.* 2008;16(7):1501-9.
14. Nikolaidis LA, Mankad S, Sokos GG, Miske G, Shah A, Elahi D, and Shannon RP. Effects of glucagon-like peptide-1 in patients with acute myocardial infarction and left ventricular dysfunction after successful reperfusion. *Circulation.* 2004;109(8):962-5.
15. Ryan GJ, and Hardy Y. Liraglutide: once-daily GLP-1 agonist for the treatment of type 2 diabetes. *Journal of clinical pharmacy and therapeutics.* 2011;36(3):260-74.
16. Valverde I, Morales M, Clemente F, Lopez-Delgado MI, Delgado E, Perea A, and Villanueva-Penacarrillo ML. Glucagon-like peptide 1: a potent glycogenic hormone. *FEBS letters.* 1994;349(2):313-6.
17. Villanueva-Penacarrillo ML, Alcantara AI, Clemente F, Delgado E, and Valverde I. Potent glycogenic effect of GLP-1(7-36)amide in rat skeletal muscle. *Diabetologia.* 1994;37(11):1163-6.
18. Galera C, Clemente F, Alcantara A, Trapote MA, Perea A, Lopez-Delgado MI, Villanueva-Penacarrillo ML, and Valverde I. Inositolphosphoglycans and diacylglycerol are possible mediators in the glycogenic effect of GLP-1(7-36)amide in BC3H-1 myocytes. *Cell biochemistry and function.* 1996;14(1):43-8.
19. Bode B. Liraglutide: a review of the first once-daily GLP-1 receptor agonist. *The American journal of managed care.* 2011;17(2 Suppl):S59-70.
20. Garber A, Henry RR, Ratner R, Hale P, Chang CT, Bode B, and Group L-S. Liraglutide, a once-daily human glucagon-like peptide 1 analogue, provides sustained improvements in glycaemic control and weight for 2 years as monotherapy compared with glimepiride in patients with type 2 diabetes. *Diabetes, obesity & metabolism.* 2011;13(4):348-56.
21. Liu Y, Wan Q, Guan Q, Gao L, and Zhao J. High-fat diet feeding impairs both the expression and activity of AMPKa in rats' skeletal muscle. *Biochemical and biophysical research communications.* 2006;339(2):701-7.
22. Dong H, Lu FE, and Gao ZQ. [Experimental study on effects of emodin

on nonalcoholic fatty liver induced by high fat diet in rats]. *Zhongguo Zhong xi yi jie he za zhi Zhongguo Zhongxiyi jiehe zazhi = Chinese journal of integrated traditional and Western medicine / Zhongguo Zhong xi yi jie he xue hui, Zhongguo Zhong yi yan jiu yuan zhu ban.* 2006;26 Suppl(64-7.

23. Satoh H, Audrey Nguyen MT, Kudoh A, and Watanabe T. Yacon diet (Smallanthus sonchifolius, Asteraceae) improves hepatic insulin resistance via reducing Trb3 expression in Zucker fa/fa rats. *Nutrition & diabetes.* 2013;3(e70.
24. Sugii H, Matsumura Y, Inoue A, Horigome H, Matsuzaki K, and Shimizu A. [Pharmacological and clinical profiles of a human GLP-1 analogue, liraglutide (Victoza((R)))]. *Nihon yakurigaku zasshi Folia pharmacologica Japonica.* 2010;136(4):233-41.
25. Cummings BP, Stanhope KL, Graham JL, Baskin DG, Griffen SC, Nilsson C, Sams A, Knudsen LB, Raun K, and Havel PJ. Chronic administration of the glucagon-like peptide-1 analog, liraglutide, delays the onset of diabetes and lowers triglycerides in UCD-T2DM rats. *Diabetes.* 2010;59(10):2653-61.
26. Satoh H, Nguyen MT, Miles PD, Imamura T, Usui I, and Olefsky JM. Adenovirus-mediated chronic "hyper-resistinemia" leads to in vivo insulin resistance in normal rats. *The Journal of clinical investigation.* 2004;114(2):224-31.
27. Satoh H, Nguyen MT, Trujillo M, Imamura T, Usui I, Scherer PE, and Olefsky JM. Adenovirus-mediated adiponectin expression augments skeletal muscle insulin sensitivity in male Wistar rats. *Diabetes.* 2005;54(5):1304-13.
28. Steele R. Influences of glucose loading and of injected insulin on hepatic glucose output. *Annals of the New York Academy of Sciences.* 1959;82(420-30.
29. Saltiel AR, and Kahn CR. Insulin signalling and the regulation of glucose and lipid metabolism. *Nature.* 2001;414(6865):799-806.
30. Towler MC, and Hardie DG. AMP-activated protein kinase in metabolic control and insulin signaling. *Circulation research.* 2007;100(3):328-41.
31. Chen H, Montagnani M, Funahashi T, Shimomura I, and Quon MJ. Adiponectin stimulates production of nitric oxide in vascular

endothelial cells. *The Journal of biological chemistry.* 2003;278(45):45021-6.

32. Drucker DJ. The biology of incretin hormones. *Cell metabolism.* 2006;3(3):153-65.
33. He L, Sabet A, Djedjos S, Miller R, Sun X, Hussain MA, Radovick S, and Wondisford FE. Metformin and insulin suppress hepatic gluconeogenesis through phosphorylation of CREB binding protein. *Cell.* 2009;137(4):635-46.
34. Gupta NA, Mells J, Dunham RM, Grakoui A, Handy J, Saxena NK, and Anania FA. Glucagon-like peptide-1 receptor is present on human hepatocytes and has a direct role in decreasing hepatic steatosis in vitro by modulating elements of the insulin signaling pathway. *Hepatology.* 2010;51(5):1584-92.
35. Ben-Shlomo S, Zvibel I, Shnell M, Shlomai A, Chepurko E, Halpern Z, Barzilai N, Oren R, and Fishman S. Glucagon-like peptide-1 reduces hepatic lipogenesis via activation of AMP-activated protein kinase. *Journal of hepatology.* 2011;54(6):1214-23.
36. Zang M, Zuccollo A, Hou X, Nagata D, Walsh K, Herscovitz H, Brecher P, Ruderman NB, and Cohen RA. AMP-activated protein kinase is required for the lipid-lowering effect of metformin in insulin-resistant human HepG2 cells. *The Journal of biological chemistry.* 2004;279(46):47898-905.
37. Iglesias MA, Ye JM, Frangioudakis G, Saha AK, Tomas E, Ruderman NB, Cooney GJ, and Kraegen EW. AICAR administration causes an apparent enhancement of muscle and liver insulin action in insulin-resistant high-fat-fed rats. *Diabetes.* 2002;51(10):2886-94.
38. Kim YD, Park KG, Lee YS, Park YY, Kim DK, Nedumaran B, Jang WG, Cho WJ, Ha J, Lee IK, et al. Metformin inhibits hepatic gluconeogenesis through AMP-activated protein kinase-dependent regulation of the orphan nuclear receptor SHP. *Diabetes.* 2008;57(2):306-14.
39. Lee JM, Seo WY, Song KH, Chanda D, Kim YD, Kim DK, Lee MW, Ryu D, Kim YH, Noh JR, et al. AMPK-dependent repression of hepatic gluconeogenesis via disruption of CREB.CRTC2 complex by orphan nuclear receptor small heterodimer partner. *The Journal of biological chemistry.* 2010;285(42):32182-91.

40. Martinez de Morentin PB, Varela L, Ferno J, Nogueiras R, Dieguez C, and Lopez M. Hypothalamic lipotoxicity and the metabolic syndrome. *Biochimica et biophysica acta.* 2010;1801(3):350-61.
41. Lam TK, van de Werve G, and Giacca A. Free fatty acids increase basal hepatic glucose production and induce hepatic insulin resistance at different sites. *American journal of physiology Endocrinology and metabolism.* 2003;284(2):E281-90.
42. Horton JD. Sterol regulatory element-binding proteins: transcriptional activators of lipid synthesis. *Biochemical Society transactions.* 2002;30(Pt 6):1091-5.
43. Shimano H. Sterol regulatory element-binding proteins (SREBPs): transcriptional regulators of lipid synthetic genes. *Progress in lipid research.* 2001;40(6):439-52.
44. Zhou G, Myers R, Li Y, Chen Y, Shen X, Fenyk-Melody J, Wu M, Ventre J, Doebber T, Fujii N, et al. Role of AMP-activated protein kinase in mechanism of metformin action. *The Journal of clinical investigation.* 2001;108(8):1167-74.
45. Holmes BF, Sparling DP, Olson AL, Winder WW, and Dohm GL. Regulation of muscle GLUT4 enhancer factor and myocyte enhancer factor 2 by AMP-activated protein kinase. *American journal of physiology Endocrinology and metabolism.* 2005;289(6):E1071-6.
46. Fryer LG, Foufelle F, Barnes K, Baldwin SA, Woods A, and Carling D. Characterization of the role of the AMP-activated protein kinase in the stimulation of glucose transport in skeletal muscle cells. *The Biochemical journal.* 2002;363(Pt 1):167-74.

FIGURE LEGENDS

Fig. 1. Shematic representation of this experiment procedure

The flowchart shows process leading to perform experiments. Male Wistar rats were fed a NCD or HFD for 3 weeks, and then were implanted with catheters. After the surgery, the rats were subsequently injected subcutaneously with normal saline or the indicated once-daily dosage of liraglutide for 7 days. After the 7-day regimen of daily injections, euglycemic hyperinsulinemic clamp or iv-GTT were performed

Fig. 2. Intravenous glucose tolerance test (iv-GTT) and insulin sensitivity during euglycemic-hyperinsulinemic clamp studies in the NCD-fed rats injected with liraglutide once daily for 7 days.

(A) Iv-GTTs were performed on the NCD-fed rats. Glucose curves are shown from the iv-GTT in NCD-fed control rats (◊; n = 4) and NCD-fed rats receiving liraglutide (0.05 mg/day: ■; n = 4, 0.10 mg/day:▲; n = 3), which were injected with glucose (2 g/kg body weight) following an 8-hour fast. Blood samples were collected from the carotid artery at 0, 15, 30, 60, 90, and 120 minutes post-glucose injection. (B) Data represent the GIR during euglycemic-hyperinsulinemic clamp studies in NCD-fed control rats (□; n = 9), and NCD-fed rats receiving liraglutide (■; 0.025 mg/day: n = 8, 0.05 mg/day: n = 10, 0.10 mg/day: n = 7). (C) Data represent the IS-GIR during euglycemic-hyperinsulinemic clamp studies in NCD-fed control rats (□; n = 9), and NCD-fed rats receiving liraglutide (■; 0.025 mg/day: n = 8, 0.05 mg/day: n = 10, 0.10 mg/day: n = 7). (D) Data represent the basal HGO in NCD-fed control rats (□; n = 9), and NCD-fed rats receiving liraglutide (■; 0.025 mg/day: n = 8, 0.05 mg/day: n = 10, 0.10 mg/day: n = 7). (E) Data represent the cHGO during euglycemic-hyperinsulinemic clamp studies in NCD-fed control rats (□; n = 9), and NCD-fed rats receiving liraglutide (■; 0.025 mg/day: n = 8, 0.05 mg/day: n = 10, 0.10 mg/day: n = 7). Data are means ± SE. *: $P < 0.05$; **:$P < 0.01$ versus the control rats. Control rats were received saline once daily.

Fig. 3. Iv-GTT and insulin sensitivity during euglycemic-hyperinsulinemic clamp studies in the HFD fed rats injected with liraglutide once daily for 7 days.

(A) Iv-GTTs were performed on the HFD fed rats. Glucose curves are shown

from the iv-GTT in HFD-fed control rats (◊; n = 8), and HFD-fed rats receiving liraglutide (0.05 mg/day: ■; n = 5, 0.10 mg/day:▲; n = 5), which were injected with glucose (2 g/kg body weight) following an 8-hour fast. Blood samples were collected from the carotid artery at 0, 15, 30, 60, 90, and 120 minutes post-glucose injection. (B) Data represent the GIR during euglycemic-hyperinsulinemic clamp studies in HFD-fed control rats (□; n = 11), and HFD-fed rats receiving liraglutide (■; 0.025 mg/day: n = 8, 0.05 mg/day: n = 8, 0.10 mg/day: n = 8). (C) Data represent the IS-GIR during euglycemic-hyperinsulinemic clamp studies in HFD-fed control rats (□; n = 11), and HFD-fed rats receiving liraglutide (■; 0.025 mg/day: n = 8, 0.05 mg/day: n = 8, 0.10 mg/day: n = 8). (D) Data represent the basal HGO in HFD-fed control rats (□; n = 11), and HFD-fed rats receiving liraglutide (■; 0.025 mg/day: n = 8, 0.05 mg/day: n = 8, 0.10 mg/day: n = 8). (E) Data represent the clamp HGO during euglycemic-hyperinsulinemic clamp studies in HFD-fed control rats (□; n = 11), and HFD-fed rats receiving liraglutide (■; 0.025 mg/day: n = 8, 0.05 mg/day: n = 8, 0.10 mg/day: n = 8). Values are means ± SE. *: $P < 0.05$; **:$P < 0.01$ versus the control rats. Control rats were received saline once daily.

Fig. 4. Akt phosphorylation (Ser473) (A and C), and AMPK phosphorylation (Thr172) (B and D), in liver, skeletal muscle, and adipose tissue samples from both NCD-fed (A and B) and the HFD-fed (C and D) rats receiving a 7-day regimen of once-daily liraglutide injections.

Basal and insulin clamp-stimulated liver, skeletal muscle, and adipose tissue samples in the NCD-fed control rats (□; basal: n = 4, clamp: n = 4), NCD-fed rats receiving 0.05mg/day liraglutide (■; basal: n = 4, clamp: n = 4), in the HFD-fed control rats (□; basal: n = 4, clamp: n = 4), and HFD-fed rats receiving 0.05mg/day liraglutide (■; basal: n = 4, clamp: n = 4) were obtained and homogenized as described in the RESEARCH DESIGN AND METHODS. The resulting homogenates were immunoblotted for phosphorylated Akt (pAkt) (Ser473), Akt, phosphorylated AMPK (pAMPK) (Thr172), and β-actin antibodies. The bar graphs show data quantification by image J software for the results from liver, skeletal muscle, and adipose tissue. Values are means ± SE. Data are expressed relative to control values. *: $P < 0.05$ versus the control rats. Control rats were received saline once daily.

Fig. 5. Gluconeogenic (G6pase (A)) and lipogenic (Fas (B), Acc (C), Acl (D), Scd-1 (E), and Srebp-1c (F)) expression during euglycemic-hyperinsulinemic clamp studies in liver samples, in both NCD-fed and the HFD-fed rats receiving a 7-day regimen of once-daily liraglutide injection.

Total RNAs extracted from liver tissues in the control rats (□; NCD-fed rats: n = 6, HFD-fed rats: n = 6) and the liraglutide-treated rats (■; NCD-fed rats: n = 6, HFD-fed rats: n = 6) were used in the analysis of G6pase (A), Fas (B), Acc (C), Acl (D), Scd-1 (E), and Srebp-1c (F) expression. Levels of Cyclophilin A (Cph) were used for normalization of sample loading. Values are means ± SEM. Data are expressed relative to control values. *: $P < 0.05$; versus control rats. Control rats were received saline once daily.

Fig. 6. GLP-1 receptor expression in liver samples, in both NCD-fed and the HFD-fed rats receiving a 7-day regimen of once-daily liraglutide injection.

Total RNAs extracted from liver tissues in the control rats (□; NCD-fed rats: n = 6, HFD-fed rats: n = 6) and the liraglutide-treated rats (■; NCD-fed rats: n = 6, HFD-fed rats: n = 6) were used in the analysis of GLP-1 receptor expression. Levels of Cyclophilin A (Cph) were used for normalization of sample loading. Values are means ± SEM. Data are expressed relative to control values. Control rats were received saline once daily.

Fig. 7. Lipid accumulation in liver samples from NCD-fed and HFD-fed rats receiving a 7-day regimen of once-daily liraglutide injections.

Basal liver tissue samples in the NCD-fed and HFD-fed rats receiving saline and 0.05 mg/day liraglutide were obtained. (A) Macroscopic images of livers. (B) Liver sections stained with Hematoxylin-eosin (H &E). (C) Liver sections stained with Oil red O.

Fig. 8. The relationship between body weight and GIR in NCD-fed (A) and HFD-fed (B) rats receiving a 7-day regimen of once-daily liraglutide injectioons.

(A) The solid and dotted regression lines represent the relationship between body weight and GIR in the NCD-fed rats receiving liraglutide (n = 25), and the control NCD-fed rats (n = 9), respectively. (B) The solid and dotted regression lines represent the relationship between body weight and GIR in the HFD-fed rats receiving liraglutide (n = 24), and the control HFD-fed rats

(n = 11), respectively. Control rats were received saline once daily.

Table 1
Plasma measurements in the basal state and during euglycemic-hyperinsulinemic clamps in NCD-fed rats.

Normal Chow Diet		Control group (*n*)	Liraglutide group		
			0.025 mg/day	0.050 mg/day	0.100 mg/day
BW (g)	Pre*	259.4±3.8(25)	268.2±4.0(8)	262.3±4.4(25)	266.6±4.3(10)
	Post*	292.6±4.8 (25)	277.6±7.9 (8)*	253.1±5.3 (25)*	234.1±7.0 (10)*
Basal state					
Glucose (mg/dl)		181.4±6.6 (12)	144.6± 4.9 (8)*	163.4±6.1 (12)*	151.0±5.3 (10)*
Insulin (ng/ml)		5.4± (12)	N.D.	3.0±0.5 (12)*	N.D.
HOMA-IR		2.5±0.4 (12)	N.D.	1.2±0.27 (12)*	N.D.
Glucagon (pg/ml)		63.1±5.5 (6)	N.D.	53.3±6.5 (6)	N.D.
TC (mg/dl)		57.0±2.5 (6)	N.D.	56.6±3.0 (6)	N.D.
TG (mg/dl)		126.6±23.0 (6)	N.D.	33.6±6.3 (6)*	N.D.
HDL-C (mg/dl)		21.3±0.7 (6)	N.D.	18.5±0.5 (6)*	N.D.
Adiponectin (μg/ml)		1.48±0.07 (6)	N.D.	1.46±0.09 (6)	N.D.
Clamp state					
Glucose (mg/dl)		149.0±2.1 (9)	146.5±2.0 (8)	147.3±4.5 (10)	148.9±1.8 (7)
Insulin (ng/ml)		876.0±47.1 (6)x	N.D.	943.3±134.3 (6)	N.D.

Control rats were received saline once daily. Basal state means a state just before euglycemic-hyperinsulinemic clamp experiments. Clamp state means a state at terminal stage of euglycemic-hyperinsulinemic clamp experiments. Pre* means pre-treatment of saline or liraglutide. Post* means post-treatment of saline or liraglutide. Statistical difference between two groups was assessed by t-test. *: $P < 0.05$, compared with control group.

Table 2
Plasma measurements in the basal state and during euglycemic-hyperinsulinemic clamps in HFD-fed rats.

High Fat Diet		Control group (*n*)	Liraglutide group		
			0.025 mg/day	0.050 mg/day	0.100 mg/day
BW (g)	Pre*	396.7±6.0(30)	388.2±12.8(8)	429.1±7.0(25)*	424.3±8.5(13)*
	Post*	413.8±7.5 (30)	369.1±14.3 (8)*	395.4±7.7 (25)*	373.0±8.8 (13)*
Basal state					
Glucose (mg/dl)		190.2±5.3 (11)	153.0±5.6 (8)*	154.0±3.1 (13)*	143.6±5.2 (13)*
Insulin (ng/ml)		6.5±1.0 (11)	N.D.	3.3±0.68(13)*	N.D.
HOMA-IR		3.1±0.5 (11)	N.D.	1.2±0.27 (13)*	N.D.
Glucagon (pg/ml)		74.3±4.6 (11)	N.D.	66.1±4.1 (13)	N.D.
TC (mg/dl)		57.1±5.1 (11)	N.D.	54.3± 2.8 (13)	N.D.
TG (mg/dl)		46.6±4.0 (11)	N.D.	31.6±3.7 (13)*	N.D.
HDL-C (mg/dl)		18.6±0.8 (11)	N.D.	15.1±0.79 (13)*	N.D.
Adiponectin (μg/ml)		1.63±0.20 (11)	N.D.	1.58±0.11 (13)	N.D.
Clamp state					
Glucose (mg/dl)		150.4±2.9 (11)	149.0±1.6 (8)	151.1±1.1 (8)	145.1±1.7 (8)
Insulin (ng/ml)		1448.0±185.1(11)	N.D.	1079.4±68.9* (8)	N.D.

Control rats were received saline once daily. Basal state means a state just before euglycemic-hyperinsulinemic clamp experiments. Clamp state means a state at terminal stage of euglycemic-hyperinsulinemic clamp experiments. Pre* means pre-treatment of saline or liraglutide. Post* means post-treatment of saline or liraglutide. Statistical difference between two groups was assessed by t-test. *: $P < 0.05$, compared with control group.

Fig. 1

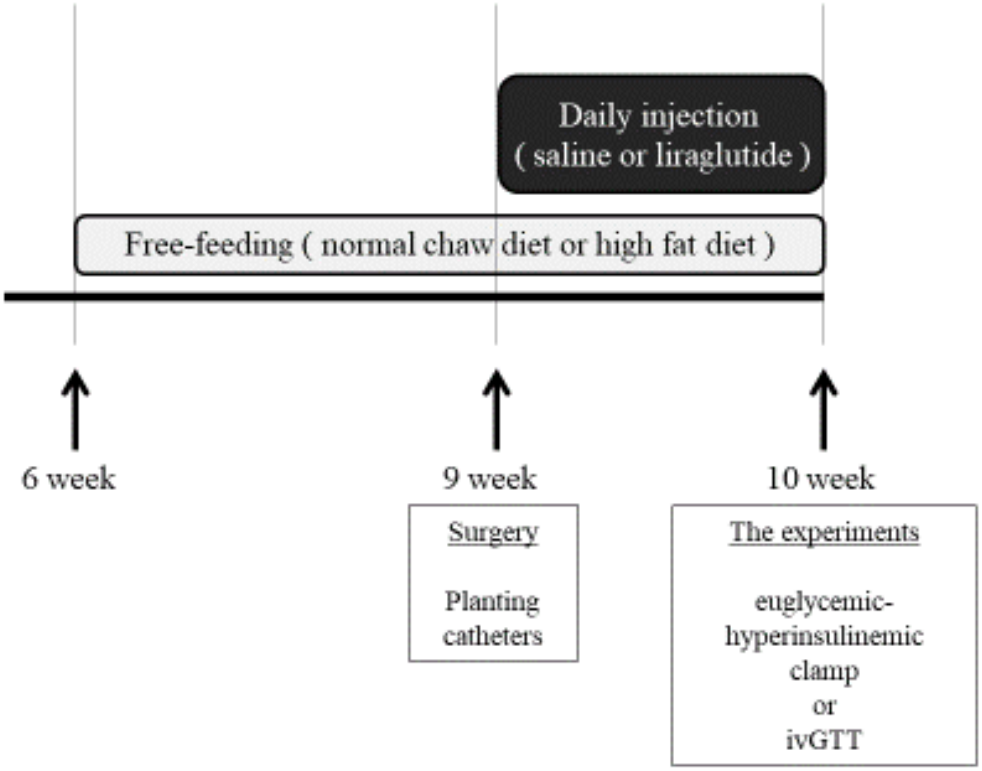
Daily injection
(saline or liraglutide)
Free-feeding (normal chaw diet or high fat diet)
6 week
9 week
10 week
Surgery
Planting
catheters
The experiments
euglycemic-
hyperinsulinemic
clamp
or
ivGTT

Fig. 2

A

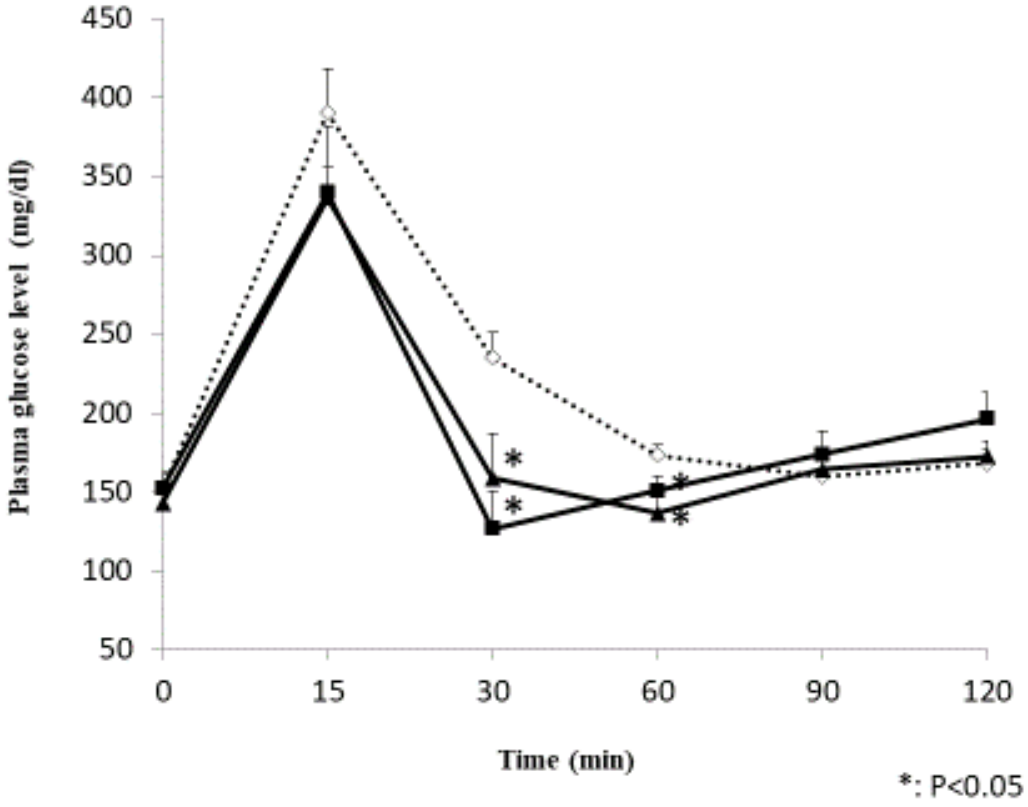
450
400
350
300
250
200
150
100
50
Plasma glucose level (mg/dl)
0
15
30
60
90
120
Time (min)
*
*
*
*
*: P<0.05

Fig. 2

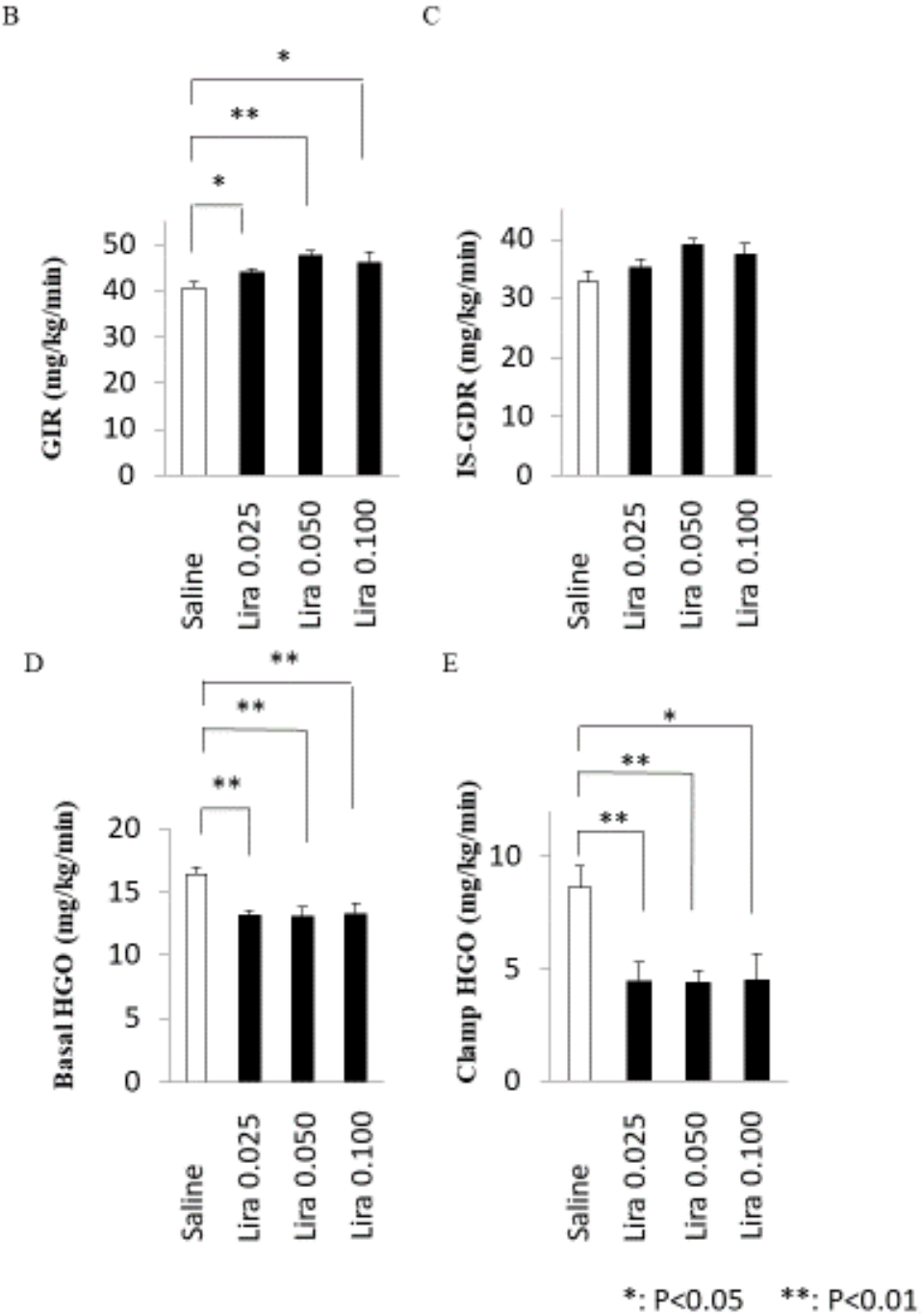
B
C
GIR (mg/kg/min)
IS-GDR (mg/kg/min)
Saline
Lira 0.025
Lira 0.050
Lira 0.100
D
E
Basal HGO (mg/kg/min)
Clamp HGO (mg/kg/min)
*: P<0.05
**: P<0.01

Fig. 3

A

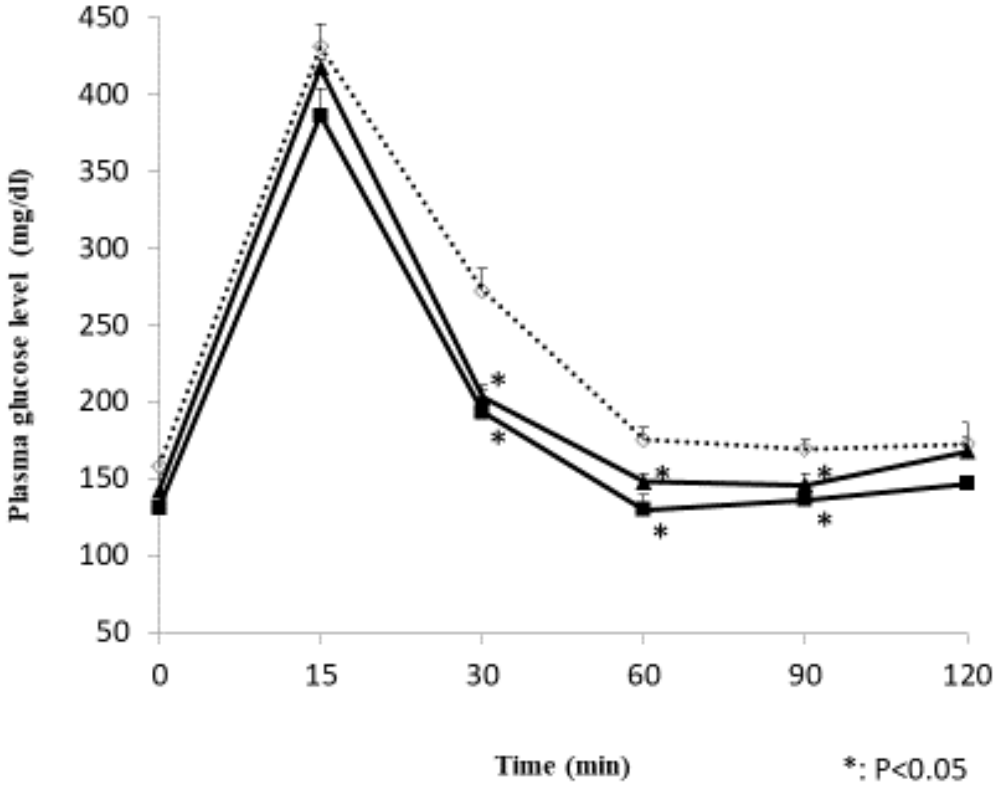
Plasma glucose level (mg/dl)
450
400
350
300
250
200
150
100
50
0
15
30
60
90
120
Time (min)
*: P<0.05

Fig. 3

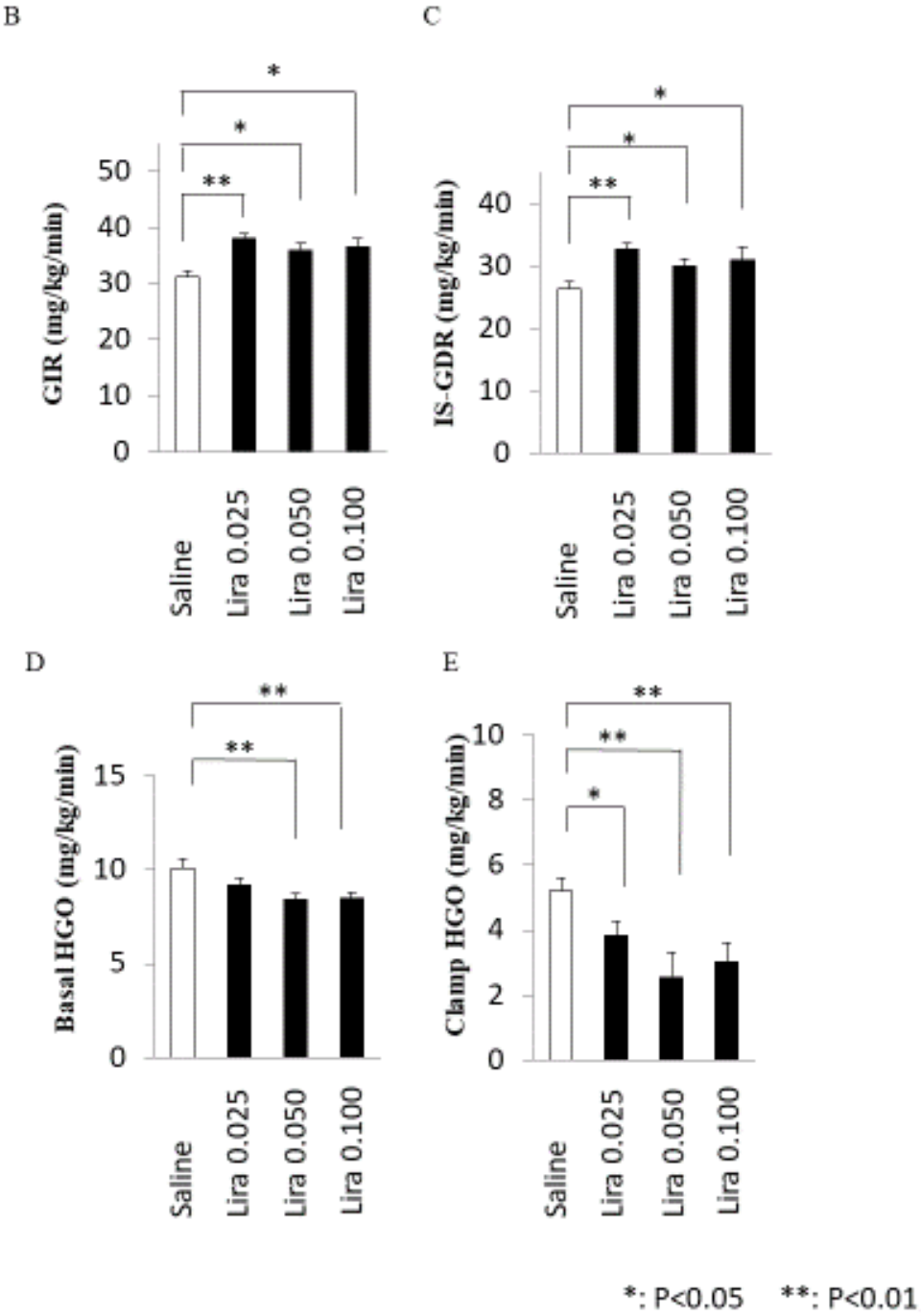
B
C
D
E
GIR (mg/kg/min)
IS-GDR (mg/kg/min)
Basal HGO (mg/kg/min)
Clamp HGO (mg/kg/min)
Saline
Lira 0.025
Lira 0.050
Lira 0.100
*: P<0.05
**: P<0.01

Fig. 4

A.

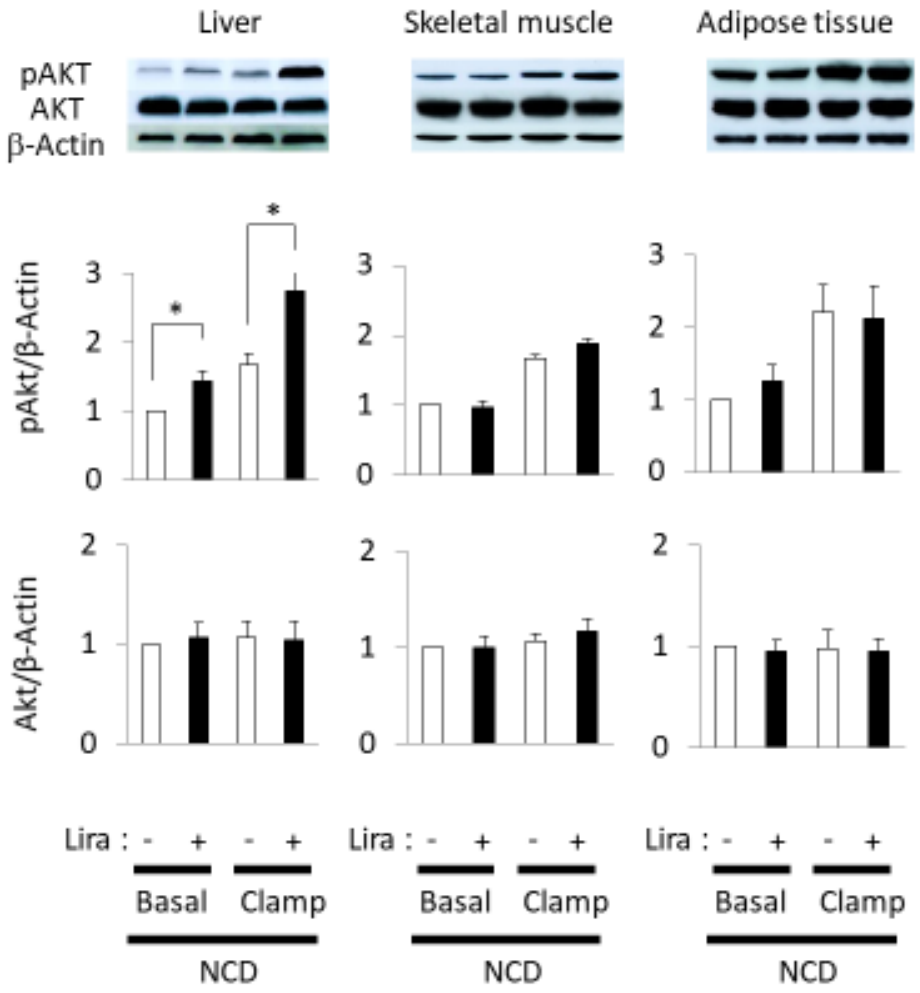
Liver
Skeletal muscle
Adipose tissue
pAKT
AKT
β-Actin
pAkt/β-Actin
Akt/β-Actin
*
*
Lira : - + - +
Basal
Clamp
NCD

*: P<0.05

Fig. 4

B.

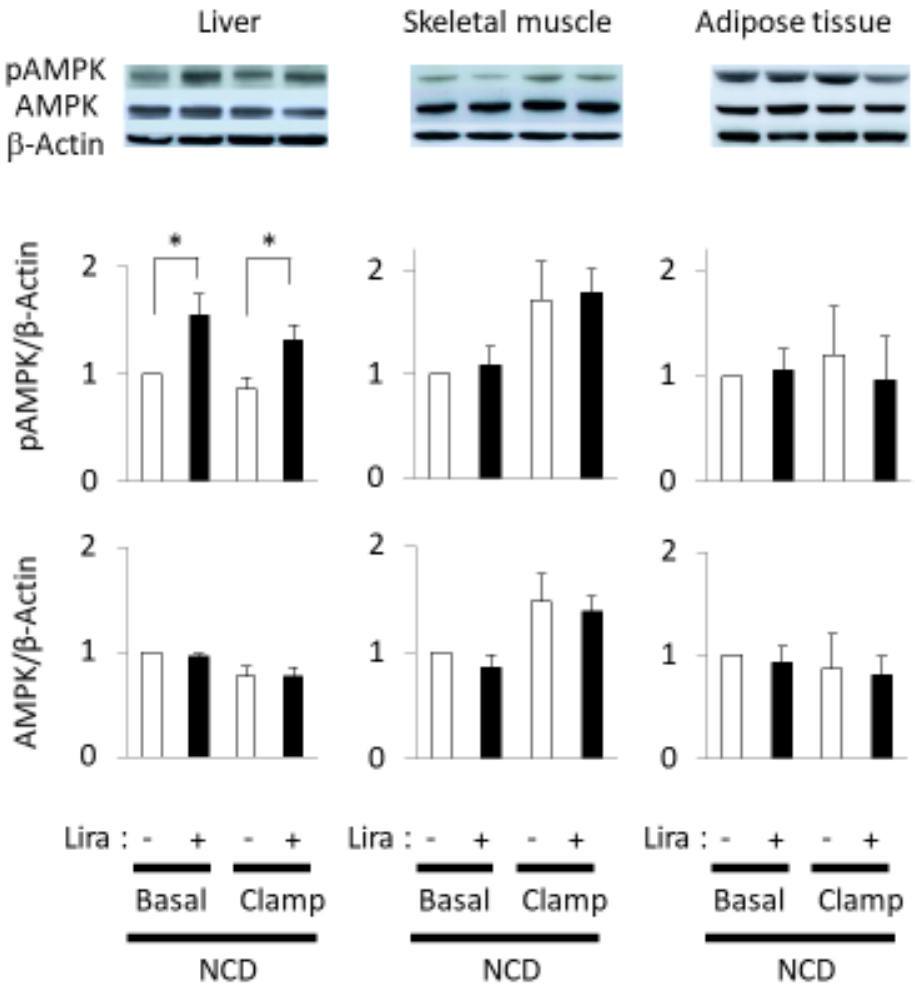
Liver
Skeletal muscle
Adipose tissue
pAMPK
AMPK
β-Actin
pAMPK/β-Actin
AMPK/β-Actin
2
1
0
*
*
Lira : - + - +
Basal
Clamp
NCD

*: P<0.05

Fig. 4

C.

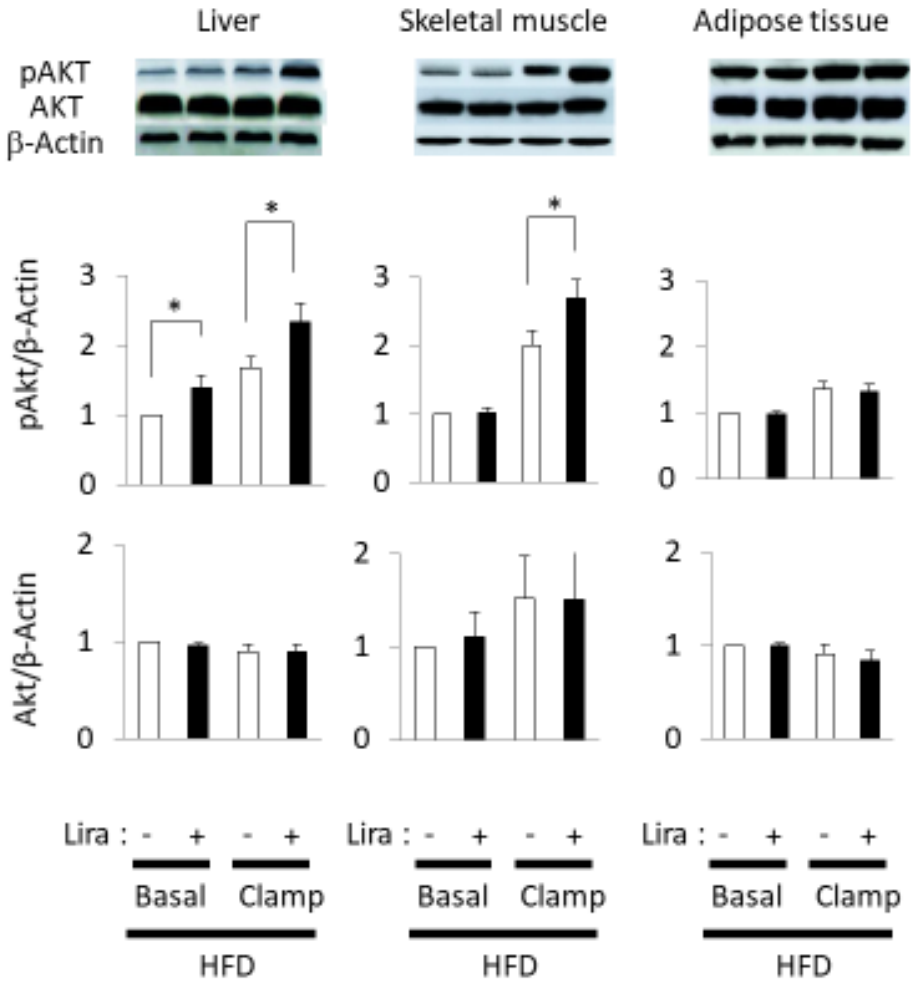
Liver
Skeletal muscle
Adipose tissue
pAKT
AKT
β-Actin
pAkt/β-Actin
Akt/β-Actin
*
Lira : - + - +
Basal
Clamp
HFD

*: P<0.05

Fig. 4

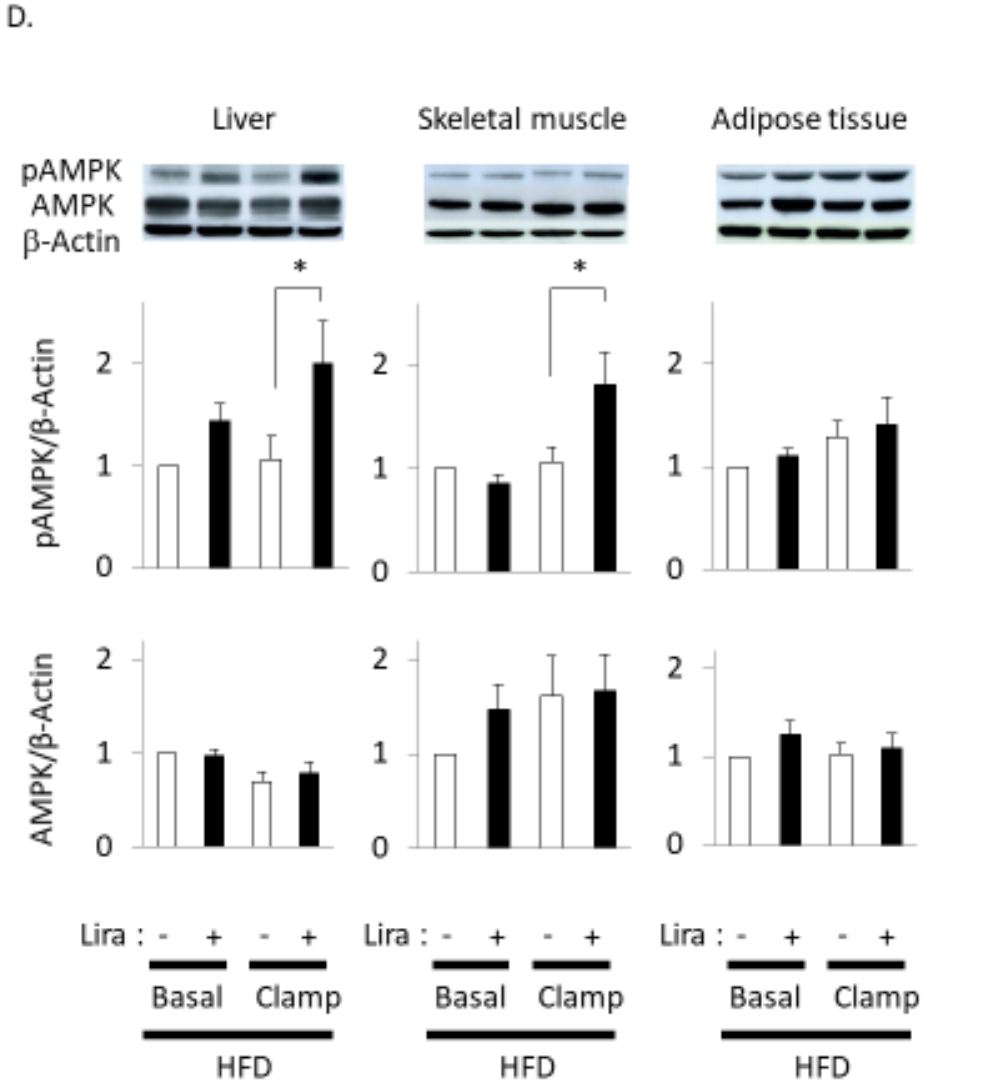
D.
Liver
Skeletal muscle
Adipose tissue
pAMPK
AMPK
β-Actin
pAMPK/β-Actin
AMPK/β-Actin
0
1
2
*
Lira : - + - +
Basal
Clamp
HFD

*: P<0.05

Fig. 5

A.

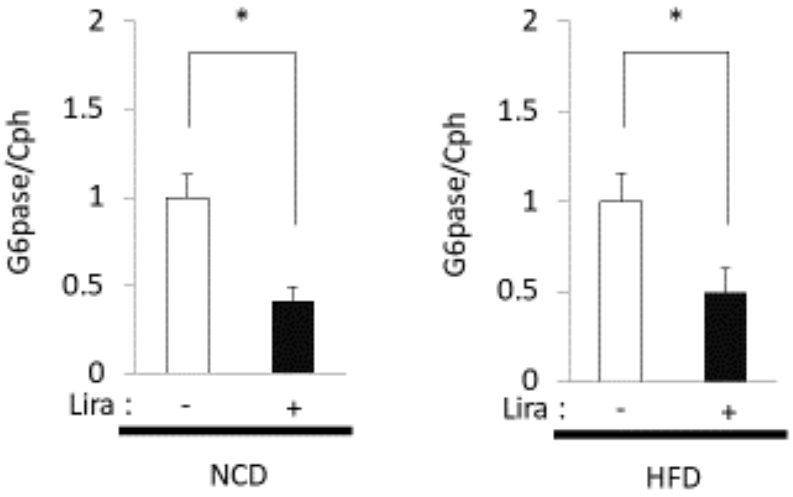

*: P<0.05

Fig. 5

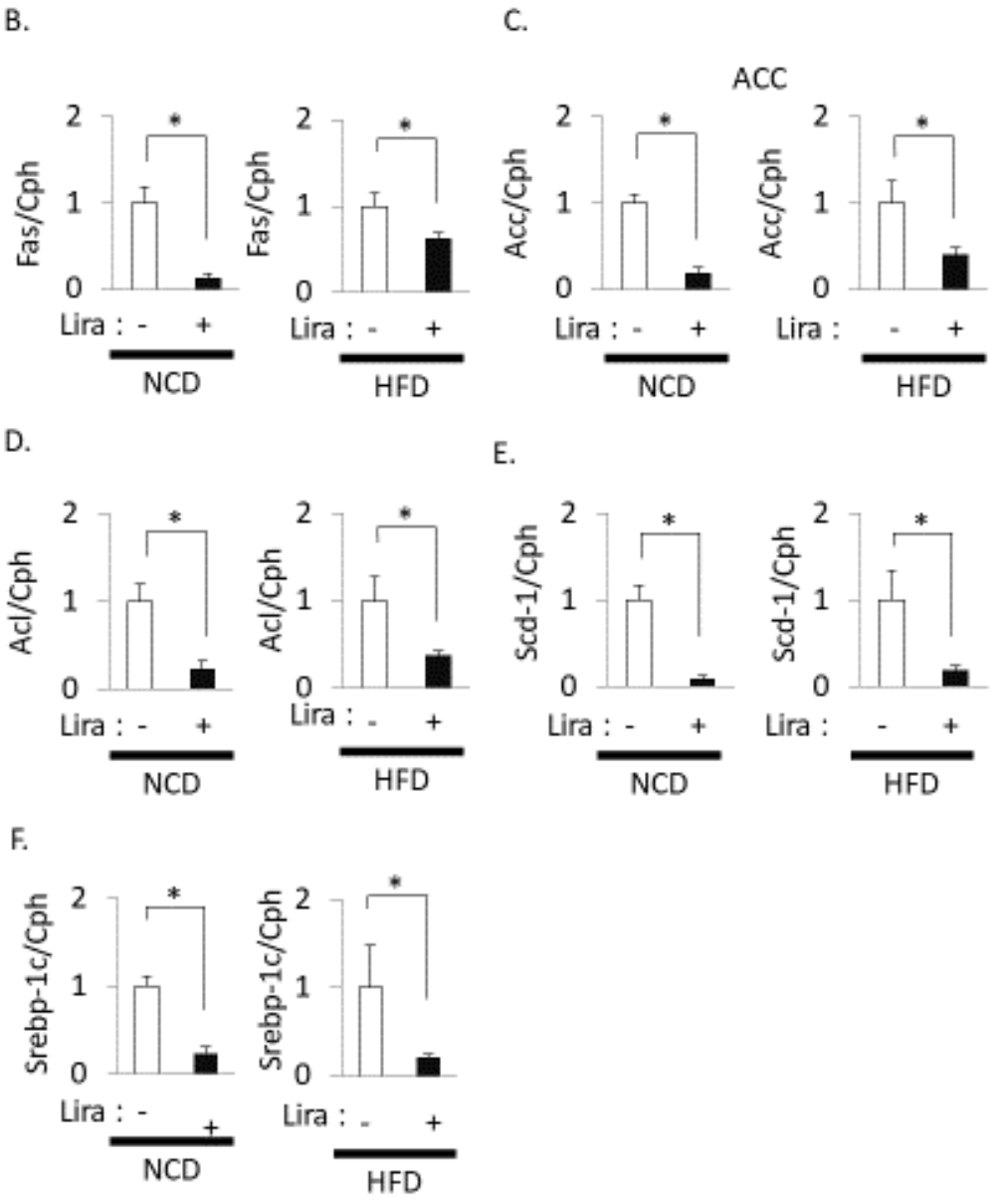
B.
C.
ACC
D.
E.
F.
Fas/Cph
Acc/Cph
Acl/Cph
Scd-1/Cph
Srebp-1c/Cph
Lira : - +
NCD
HFD
*

*: P<0.05

Fig. 6

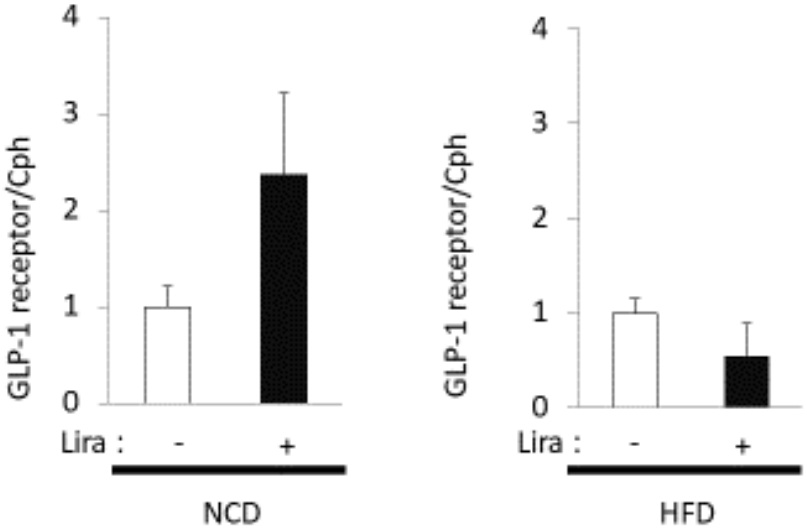
GLP-1 receptor/Cph
4
3
2
1
0
Lira : - +
NCD
GLP-1 receptor/Cph
4
3
2
1
0
Lira : - +
HFD

Fig. 7

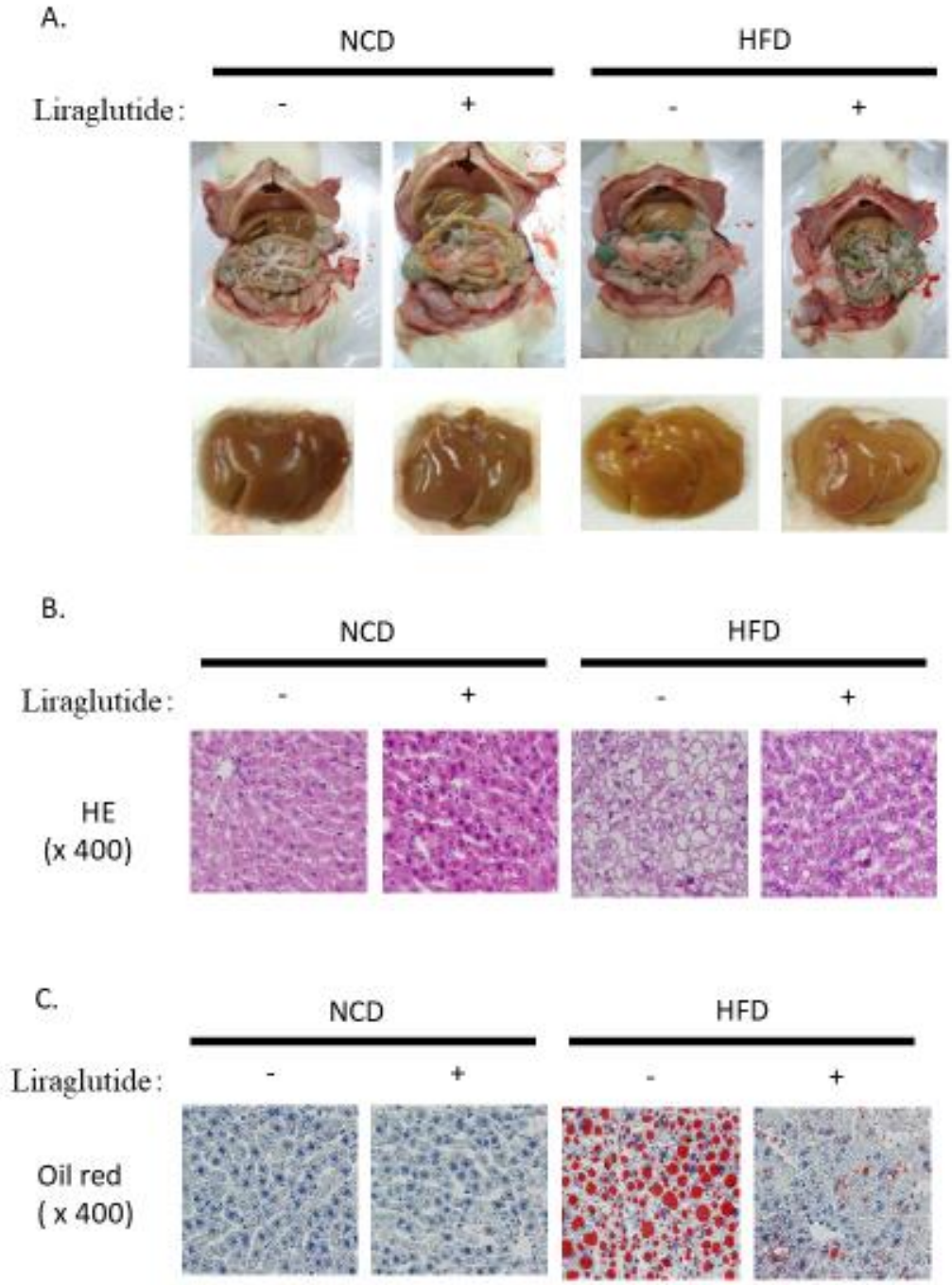
A.
NCD
HFD
Liraglutide:
-
+
-
+
B.
NCD
HFD
Liraglutide:
-
+
-
+
HE
(x 400)
C.
NCD
HFD
Liraglutide:
-
+
-
+
Oil red
(x 400)

Fig. 8

A.

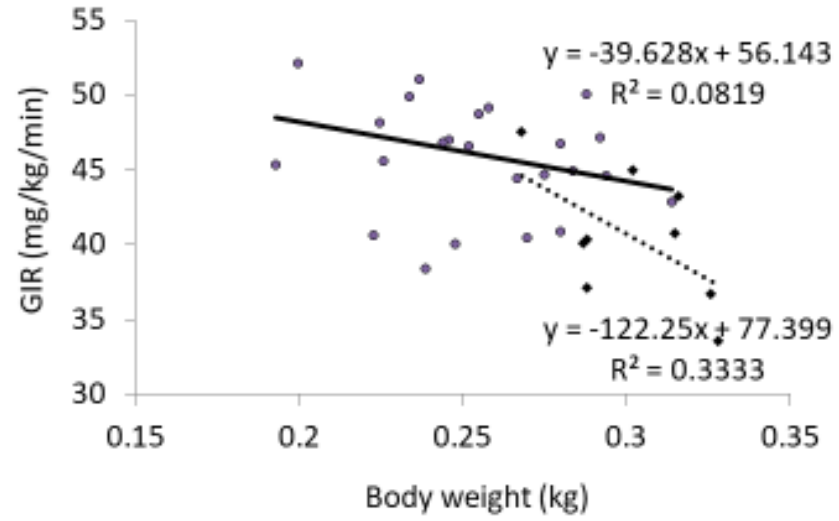
y = -39.628x + 56.143
R² = 0.0819
y = -122.25x + 77.399
R² = 0.3333
GIR (mg/kg/min)
Body weight (kg)
55
50
45
40
35
30
0.15
0.2
0.25
0.3
0.35

B.

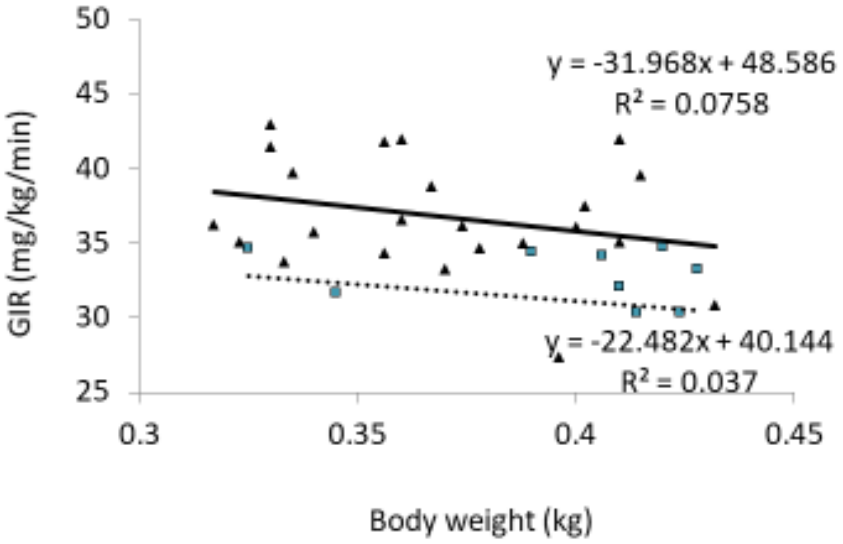
y = -31.968x + 48.586
R² = 0.0758
y = -22.482x + 40.144
R² = 0.037
GIR (mg/kg/min)
Body weight (kg)
50
45
40
35
30
25
0.3
0.35
0.4
0.45